European Journal of Radiology Open 13 (2024) 100612

Contents lists available at ScienceDirect

European Journal of Radiology Open

journal homepage: www.elsevier.com/locate/ejro

Coronary CT angiography: First comparison of model-based and hybrid iterative reconstruction with the reference standard invasive catheter angiography for CAD-RADS reporting

Aiste Matuleviciute-Stojanoska [a,*], Julia Sautier [a], Verena Bauer [c], Martin Nuessel [a], Volha Nizhnikava [b], Christian Stumpf [c], Thorsten Klink [a]

[a] Institute of Diagnostic and Interventional Radiology, Klinikum Bayreuth, Medical Campus Oberfranken, Friedrich Alexander University Erlangen, Bayreuth, Germany
[b] Department of Radiology, Kantonsspital Graubuenden, Chur, Switzerland
[c] Department of Cardiology, Klinikum Bayreuth, Medical Campus Oberfranken, Friedrich Alexander University Erlangen, Bayreuth, Germany

HIGHLIGHTS

- IMR offers superior image quality and more precise measurements than HIR.
- IMR demonstrates stronger correlation with ICA in comparison to HIR.
- IMR shows high correlation between automatic and manual evaluations of stenosis.
- IMR increases diagnostic accuracy in obese patients compared to HIR.

ARTICLE INFO

Keywords:
Coronary CTA
Iterative model-based reconstruction (IMR)
Hybrid iterative reconstruction (HIR)
Diagnostic accuracy
Plaque analysis
Obesity

ABSTRACT

Background: The purpose of this study was to compare CCTA images generated using HIR and IMR algorithm with the reference standard ICA, and to determine to what extend further improvements of IMR over HIR can be expected.
Methods: This retrospective study included 60 patients with low to intermediate CAD risk, who underwent coronary CTA (with HIR and IMR) and ICA. ICA was used as reference standard. Two independent and blinded readers evaluated 2226 segments, classifying stenosis with CAD-RADS (significant stenosis $\geq$3). Image quality was assessed with a 5-point scale, SNR in the ascending aorta, and FWHM of proximal LCA calibers. The impact of image noise, radiation dose, and BMI on diagnostic accuracy was evaluated using ROC curves and Fisher's Exact Test. Quantitative plaque analysis was performed on 28 plaques.
Results: IMR showed higher image quality than HIR (IMR 4.4, HIR 3.97, $p<0.001$) with better SNR (21.4 vs. 13.28, $p<0.001$) and FWHM (4.44 vs. 4.55, $p=0.003$). IMR had better diagnostic accuracy (ROC AUC 0.967 vs. 0.948, $p=0.16$, performed better at higher radiation doses ($p=0.02$) and showed a larger minimum lumen area ($p=0.022$ and $p=0.046$).
Conclusion: IMR offers significantly superior image quality of CCTA, more precise measurements, and a stronger positive correlation with ICA. The overall diagnostic accuracy may be superior with IMR, although the differences were not statistically significant. However, in patients who are exposed to higher radiation doses during

Abbreviations: AHA, American Heart Association; BMI, body mass index; Bpm, beats per minute; CAD, coronary artery disease; CAD-RADS, Coronary Artery Disease, Reporting and Data System; CCTA, Coronary CT angiography; DLP, dose length product; FBP, filtered back projection; FWHM, Full Width Half Maximum; HIR, hybrid-Iterative reconstruction; HU, Hounsfield units; IMR, model-based iterative reconstruction; LAD, left anterior descending coronary artery; NPV, negative predictive value; PPV, positive predictive value; ROC curve, Receiver operating characteristic curve; ROI, region of interest; SCCT, Society of Cardiovascular Computed Tomography; SNR, signal to noise ratio.

* Correspondence to: Institute of Diagnostic and Interventional Radiology, Klinikum Bayreuth, Medical Campus Oberfranken, Friedrich-Alexander University Erlangen, Preuschwitzer Str. 10, Bayreuth, Bavaria 95445, Germany.
E-mail address: aiste.matuleviciute-stojanoska@klinikum-bayreuth.de (A. Matuleviciute-Stojanoska).

https://doi.org/10.1016/j.ejro.2024.100612
Received 4 August 2024; Received in revised form 16 October 2024; Accepted 10 November 2024

CCTA due to their constitution, IMR enables significantly better diagnostic accuracy than HIR thus providing a specific benefit for obese patients.

1. Introduction

Approximately 1 % of all patients contact their general practitioners due to chest complaints [1]. In patients with low to moderate pretest probability of coronary artery disease (CAD), the European and American guidelines recommend coronary CT angiography (CCTA) as the initial diagnostic test [2].

CCTA has become a widely utilized diagnostic tool and has been investigated intensively in numerous studies over the last decades. A substantial number of studies have demonstrated that CCTA is highly accurate for detecting coronary artery stenosis [3,4]. In this context, evolving new CT imaging techniques have been tested and investigated continually. The developments with most impact in literature were technical improvements of detectors and other hardware parts facilitating optimized image acquisition techniques, but also included new reconstruction algorithms. The latter included advantageous software-sided, post-processing approaches after data acquisition that improved image quality significantly, particularly by reducing undesired noise on generated images. However, not a better image quality was intended primarily, but rather the option for significant radiation dose savings where image quality is kept on constant levels.

During this developmental process, the standard image reconstruction algorithm "filtered back projection" (FBP), which has been used for many years, is replaced slowly by the new hybrid iterative reconstruction (HIR) algorithm. Nowadays, HIR has displaced FBP on many CT machines worldwide but is currently also challenged by further computational improvements, resulting in the newest generation of iterative model-based reconstruction (IMR) algorithms.

Existing IMR studies were designed for testing the feasibility of using lower tube voltages in combination with contrast material dose reductions and iterative model reconstruction [5–8]. In other works, the diagnostic performance of CCTA using different reconstruction algorithms in comparison to the standard algorithm was tested [9,10]. However, direct comparisons with the reference standard invasive catheter angiography are still pending.

The purpose of this study was to compare CCTA images generated using both the HIR and the IMR algorithm with the reference standard ICA, and to determine to what extend further improvements of IMR over HIR can be expected for diagnostic accuracy, image quality, automated post-processing, interobserver agreement, and plaque analysis.

2. Materials and methods

2.1. Study population

The requirement for approval or written informed consent for this retrospective study was waived by the institutional review board. A total of 104 patients with a low to moderate risk of CAD underwent CCTA between July 2020 and February 2022 at the Bayreuth Hospital on clinical indication according to the national guidelines [2]. Among these, 60 patients (18 women and 42 men) with a mean age of 63 (range, 43–83) years had been referred for ICA based on CCTA findings, and only these 60 patients were included in the study.

2.2. CCTA acquisition protocol

In the absence of contraindications, patients with irregular heart rhythms or heart rates >65 beats per minute (bpm) received up to 10 mg of intravenous ß-blockers (Metoprololtartrat-Omniapharm® 5 mg/5 ml, Recordati Pharma GmbH, Ulm, Germany) prior to the acquisition. In addition, all patients received two sublingual applications of nitroglycerin spray (Nitrolingual® akut® Spray 0.4 mg, Pohl-Boskamp, Hohenlockstedt, Germany) immediately before the scan.

CCTA was performed using a 256-MSCT scanner (Brilliance iCT; Philips Healthcare, Cleveland, OH, USA). All patients were scanned in the supine position with elevated arms. A weight-adjusted tube potential of 80–120 kV was used, and a volume of 70–80 ml of iodinated contrast agent (Imeron 400 or Imeron 350, Bracco Altana, Dresden, Germany) was injected intravenously with a flow rate of 4–5 ml/s, followed by 40 ml of saline at a flow rate of 4–5 ml/s. A region of interest was placed in the descending aorta for bolus tracking. A step-and-shoot scan with prospective ECG triggering and two subsequent axial acquisitions was performed for regular heart rhythm and heart rate <65 bpm. Using a collimation of 128 ×0.625 mm, the z-axis coverage was 6.24 cm per rotation. This is due to beam overlap when the z-flying focal spot is used. If the heart rhythm was irregular or the heart rate was >65 bpm, a helical scan with retrospective ECG gating was used. The CCTA was conducted according to the following parameters: 2 ×128 x 0.625 mm collimation with z-flying focal spot, 0.27 s rotation time, tube voltage 120 kVp, and effective tube current-time product 129–700 mAs with tube current modulation. All CCTA images were reconstructed using the HIR and IMR algorithms using Xres Standard Kernel for iDose4 and Cardiac Routine Kernel for IMR (iDose4 and IMR, Philips Healthcare, Cleveland, OH, USA). Axial images with prospective ECG triggering had thickness of 0.9 mm and with retrospective ECG gating of 0.8 mm without gap with a matrix of 512/512 and reconstructed field of view (FOV) of 250 mm.

Previously, the subjective image quality of a complete data set of CCTA images reconstructed at different levels of noise reduction strength of the HIR (7 levels) and IMR algorithms (3 levels) was evaluated by 3 experienced radiologists using a 5-point scale (5 - excellent, 1 - poor image quality). Best image quality was observed at level 4 (iDose level 4) for HIR and at level 1 for IMR. Therefore, these levels of the reconstruction algorithms were selected for our study evaluation, although one of the highest possible HIR levels was compared with the lowest IMR level.

The scan images were analyzed and evaluated using a standard PACS workstation (IMPAX EE, Agfa HealthCare, Belgium) and Philips Intellispace Portal, CT Comprehensive Cardiac Analysis (Philips Healthcare, Cleveland, OH, USA).

2.3. ICA

ICA was performed within 3 months after CCTA by experienced and board-certified interventional cardiologists with Siemens Healthcare Axiom Artis *(Siemens Healthineers, Forchheim, Germany)* device using standard techniques via transfemoral or transradial arterial access. The degree of the most severe stenosis of the segment was assessed visually and graded according to American Heart Association (AHA) recommendations [11].

2.4. Image analysis

2.4.1. Image quality assessment

The quality of CCTA images reconstructed using HIR and IMR was assessed subjectively using a 5-point rating scale (1 - very poor image quality, 5 - very good image quality) and objectively by measuring the signal-to-noise ratio (SNR) in the ascending aorta (SNR=mean signal value/standard deviation). The mean signal values (Hounsfield units (HU)) were measured on axial reconstructions displaying angiographic window settings (width (W) = 900–1100 HU, centre (C) = 220–400 HU) with a slice thickness of 0.675 mm, the diameter of the circular region of

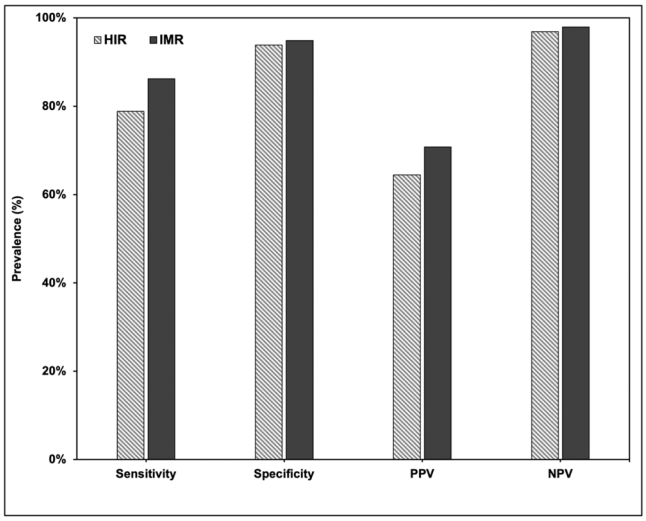

Fig. 1. Sensitivity, specificity, PPV and NPV of CCTA with HIR and IMR reconstructions of the entire study population (N=60).

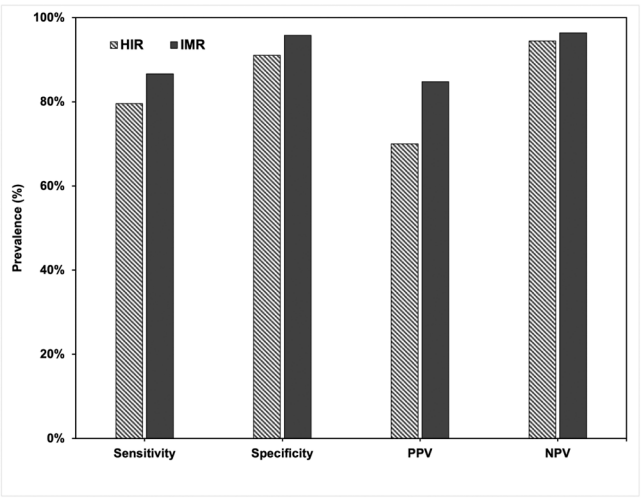

Fig. 3. Sensitivity, specificity, PPV and NPV of CCTA with HIR and IMR reconstructions with higher DLP (N=20).

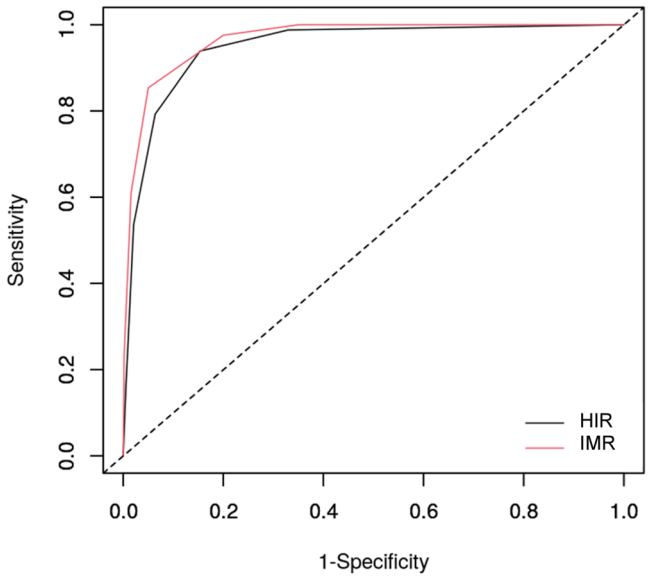

Fig. 2. ROC curves for the diagnostic accuracy of CCTA with HIR (AUC=0.95) and IMR (AUC=0.97) reconstructions of the entire study population (N=60).

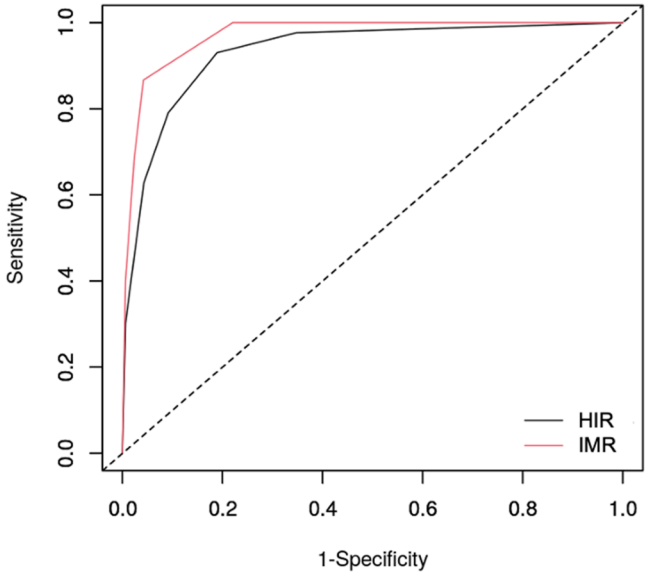

Fig. 4. ROC curves for the diagnostic accuracy of CCTA with HIR (AUC=0.93) and IMR (AUC=0.97) reconstructions with higher DLP (N=20).

interest (ROI) in the ascending aorta was >1.5 cm. Then, a more dedicated image quality analysis with focus on coronary arteries was performed by generating Full Width Half Maximum (FWHM) curves using the ImageJ software *(National Institutes of Health and the Laboratory for Optical and Computational Instrumentation, University of Wisconsin, USA)*. For this purpose, the measurement line in both reconstructions was placed at an identical position in the main trunk, the proximal LAD or the proximal LCX, perpendicular to the vessel lumen and could not be shorter than 1 cm. Resulting FWHM curves with measurements of slanted-edges was used as parameter for assessing contrast sharpness.

2.4.2. Coronary artery stenosis evaluation

Cases for the assessment of the degree of coronary artery stenosis on CCTA were randomised separately for HIR and IMR, and independently evaluated in a blinded manner by two observers. The observers were two board certified radiologists with dedicated training in CCTA reading. Segments were divided according to the 18-segment model of the Society of Cardiovascular Computed Tomography (SCCT), and stenoses were graded according to the criteria of the of the Coronary Artery Disease - Reporting and Data System (CAD-RADS)[12]. Significant stenosis was defined as CAD-RADS ≥3, i. e. stenosis ≥50 %. If a coronary artery segment had multiple stenoses, the most severe of these was evaluated.

ICA was also assessed in a blinded fashion by two experienced observers, an interventional cardiologist and an interventional radiologist with previous cardiac surgery training and used as the reference standard after consensus was reached.

2.4.3. Impact of radiation dose, image noise and BMI on the diagnostic accuracy of CCTA

To assess the influence of dose length product (DLP), SNR, and body mass index (BMI) on the diagnostic accuracy of CCTA using HIR and IMR reconstructions, the total study population of 60 patients was divided into three groups of 20, based on each criterion (one-third of the patients represented the lowest, one-third intermediate and one-third highest values for each criterion). For further calculations, only data from patients in the six most extreme groups (highest and lowest image noise,

Table 1
A comparison of quantitative plaque analysis (calcium content, maximum plaque burden, and minimum lumen area) with the HIR and IMR reconstructions, automatically (A) and after manual adjustment (H).

	(A) Automatic		(H) Manually adjusted		
	HIR A	IMR A	HIR H	IMR H	p-Value
Calcium content					
Average	81.61	83.64	91.54	89.14	
HIR A vs HIR H	81.61		91.54		p=0.015
IMR A vs IMR H		83.64		89.14	p=0.152
HIR A vs IMR A	81.61	83.64			p=0.495
HIR H vs IMR H			91.54	89.14	p=0.159
Max. plaque burden					
Average	27.79	28.43	38.36	37.89	
HIR A vs HIR H	27.79		38.36		p<0.001
IMR A vs IMR H		28.43		37.89	p<0.001
HIR A vs IMR A	27.79	28.43			p=0.575
HIR H vs IMR H			38.36	37.89	p=0.663
Min. lumen area					
Average	5.39	6.03	5.38	5.9	
HIR A vs HIR H	5.39		5.38		p=0.972
IMR A vs IMR H		6.03		5.9	p=0.6
HIR A vs IMR A	5.39	6.03			p=0.022
HIR H vs IMR H			5.38	5.9	p=0.046

DLP, and BMI) were considered.

2.4.4. Quantitative plaque analysis

Quantitative analysis of coronary plaques was performed using the Plaque Composition tool of the Philips Intellispace Portal post-processing software platform *(Philips Healthcare, Cleveland, OH, USA)*. Proximal segments of the coronary arteries (segment 1, 5, 6, and 11) with CAD-RADS 2–4 stenosis on either CCTA or ICA were included in the analysis. For the selected segments in each dataset reconstructed with HIR and IMR, automatic segmentation and calculation of the Curved Planar Reformations of the coronary arteries was performed without user interaction. The following exclusion criteria were applied to avoid misinterpretation of findings: the segments or plaques that were automatically not detected by either HIR or IMR, long-segment plaques (>1.5 cm length), two consecutive plaques automatically detected as one, or plaques located at the level of a vessel bifurcation. A total of 28 plaques (e.g., lipid, mixed, or calcified) were analyzed after the selection process. The evaluation included analysis of identical plaques with HIR and IMR reconstructions. Firstly, the automatically calculated calcium content, minimum lumen area, and maximum plaque burden were documented. Secondly, the markings of the outer vessel wall and remaining coronary lumen were manually corrected and documented once more.

2.5. Statistical analysis

Unless otherwise stated, data are displayed as mean ± standard deviation or percentages. Differences between HIR and IMR in subjective image quality, SNR, FWHM, and plaque analysis were assessed using paired t-test. In order to evaluate the diagnostic accuracy of CCTA, the CAD-RADS classification was employed to facilitate a comparison of Receiver operating characteristic (ROC) curves, sensitivity, and specificity [13]. To calculate the PPV and NPV, the prevalence of significant stenoses was compared to that of non-significant stenoses and contingency tables were used. Two independent blinded observers evaluated both CCTA and ICA, and consensus results were used for diagnostic accuracy calculations. Interobserver and inter-method agreement were tested using Cohen's kappa coefficient (κ) [14], with κ>0.8 considered perfect. Spearman's coefficient was used to assess the correlation between HIR, IMR and ICA as well as between DLP and BMI, with ρ>0.9 considered very high [15]. Fisher's exact test was used to determine the impact of DLP, SNR, and BMI on sensitivity and specificity of the HIR and IMR reconstructions [16]. Pearson's correlation coefficient was used for quantitative plaque analysis, with r>0.9 considered excellent [17]. The absolute and relative differences between automated plaque detection and manual correction were described by Bland and Altman [18]. The significance level was p≤0.05.

Unless otherwise noted, statistical analysis was performed with SPSS (version 29.0, IBM, Washington, USA).

3. Results

3.1. Image quality

The subjective image quality was 3.97 ±0.98 for HIR and 4.4 ±0.76 for IMR (p<0.001). Similarly, the objective image quality for IMR was also significantly higher than that for HIR, with an SNR of 21.4 ±5.52 for IMR vs 13.3 ±4.05 for HIR (p<0.001). Furthermore, IMR exhibited significantly steeper curves and lower FWHM values than HIR (FWMH of HIR 4.55 ±0.81 vs of IMR 4.44 ±0.77; p=0.003), which were associated with superior image quality and sharper image.

3.2. Diagnostic accuracy of CCTA

According to the 18-segment-modell, a total of 1080 segments of the coronary arteries from 60 patients were included in the study (1080 with HIR, 1080 with IMR and 1080 in ICA). Due to the variability of the distal segments, it is expected that not all of the 18 segments are present at each patient. The following exclusion criteria were applied: segments that were not present or not assessable due to their short length (237 segments, 21.9 % with HIR and 231 segments, 21.4 % with IMR), thin segments with a diameter <1.8 mm (105 segments, 9.72 % with HIR and 104 segments, 9.63 % with IMR), segments with motion artifacts (31 segments, 2.87 % with HIR and 45 segments, 4.17 % with IMR), and stented segments (5 segments, 0.46 % with HIR and IMR).

Finally, 693 segments with HIR and 695 with IMR were included in the study and evaluated by two observers. Of these, a total of 514 segments with HIR and 482 segments with IMR were detected automatically by the Comprehensive Cardiac Analysis tool of the Philips IntelliSpace Portal post-processing platform. The remaining 179 segments with HIR and 213 segments with IMR that had not been recognized automatically were marked manually. In addition, a total of 838 segments of the coronary arteries in the ICA were evaluated by two observers.

The segment-based evaluation demonstrated excellent diagnostic accuracy of CCTA with both HIR and IMR reconstructions. Sensitivity, specificity, PPV, and NPV were found to be 78.8 %, 93.8 %, 64.4 %, and 96.9 %, respectively, using HIR, and 86.2 %, 94.9 %, 70.8 %, and 97.9 %, respectively, using IMR (Fig. 1). The area under the ROC curve was 0.948 with HIR and 0.967 with IMR (Fig. 2). However, this difference was not statistically significant (p=0.16, according to DeLong et al. [19]). A high positive correlation was observed between IMR and ICA, with a correlation coefficient of 0.746 (p<0.001) and HIR demonstrated a moderate positive correlation with a correlation coefficient of 0.668 (p<0.001). The inter-method agreement was substantial for both HIR with ICA (κ=0.66, p<0.001) and IMR with ICA (κ=0.74, p<0.001), although slightly better for IMR. Moreover, the interobserver agreement was substantial for both reconstructions, although slightly superior for IMR (κ=0.68, p<0.001) in comparison to HIR (κ=0.61, p<0.001).

3.3. Impact of DLP, SNR and BMI on the diagnostic accuracy of CCTA

In the group of patients (N=20) who received a higher radiation exposure during the CCTA examination (DLP 398–833 mGy*cm), the following values were calculated: sensitivity 79.6 %, specificity 91.1 %, PPV 70 % and NPV 94.4 % with HIR reconstructions; and sensitivity 86.7 %, specificity 95.8 %, PPV 84.8 % and NPV 96.4 % with IMR reconstructions (Fig. 3). In addition, the ROC analysis demonstrated that IMR exhibited significantly superior diagnostic accuracy compared to

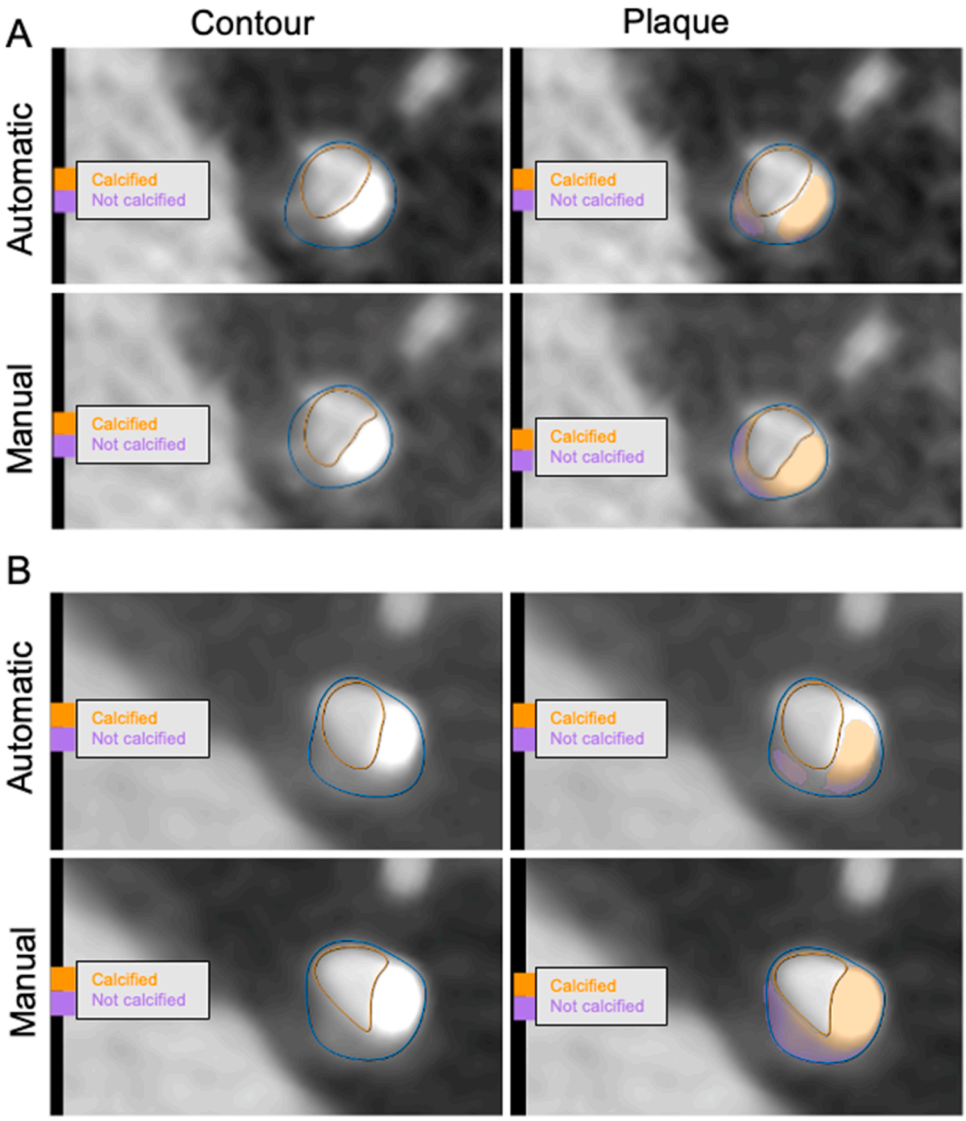

Fig. 5. Quantitative plaque/stenosis analysis. Examples of meassurements on orthogonal coronary artery images after automatic centerline angulation for lumen (left) and plaque measurements (right) using automatic and manual delineation of the outer vessel wall (blue) and the remaining contrasted vessel lumen (orange) on the HIR (A) and IMR images (B). In the plaque analysis (right), the non-calcified plaque parts are purple and the calcified parts are orange.

HIR (area under the ROC curve of HIR 0.933, of IMR 0.971, p=0.02) (Fig. 4). Moreover, the exact Fisher test demonstrated that higher DLP has a significant impact on the specificity of HIR. There was no significant impact of low DLP, SNR, or BMI on the diagnostic accuracy of CCTA with HIR or IMR. The correlation coefficient of 0.552 (p<0.001) pointed towards a moderate positive correlation between DLP and BMI.

3.4. Coronary plaque measurements

The results of the quantitative plaque analysis with HIR and IMR are presented in Table 1 and compared in Fig. 6 using Bland-Altman plots. The calcium content and maximum plaque burden were found to be significantly higher on HIR images following manual contour adjustment compared to automatic contour marking (p=0.015 and p<0.001). Furthermore, a significantly greater maximum plaque burden was observed with IMR following manual correction compared to automatic contour marking (p<0.001). The minimum lumen area was found to be significantly larger in the IMR images compared to the HIR images, both for the automatic and manual plaque marking (p=0.022 and p=0.046, respectively). Examples of automated and manual measurements of stenosis and plaque composition are demonstrated in Fig. 5. Excellent correlation of minimum lumen area between automatic and manual contour adjustments was observed with HIR (r=0.9, p<0.001), while using IMR, a slightly lower but still very strong correlation was identified (r=0.887, p<0.001). The maximum plaque burden demonstrated a very strong correlation in both reconstructions, though slightly better with IMR (r=0.803, p<0.001) than with HIR (r=0.701, p<0.001). The calcium content showed a weak correlation between automatic and manual contour markings with HIR (r=0.405, p=0.032) and a moderate correlation with IMR (r=0.521, p=0.004).

4. Discussion

In agreement with previous works [6,7], the results of our study showed that IMR reconstructions provide significantly better subjective and objective image quality compared to HIR and the standard reconstruction algorithm FBP. This is attributed particularly to reduction of image noise. Improved noise reduction rendered superior, highly positive correlation and substantial inter-method agreement between IMR and ICA, compared to HIR and ICA. In addition, IMR led to slightly better interobserver agreement than HIR. Similar results were found also in the study by Qin et al. in the assessment of renal artery stenoses [20].

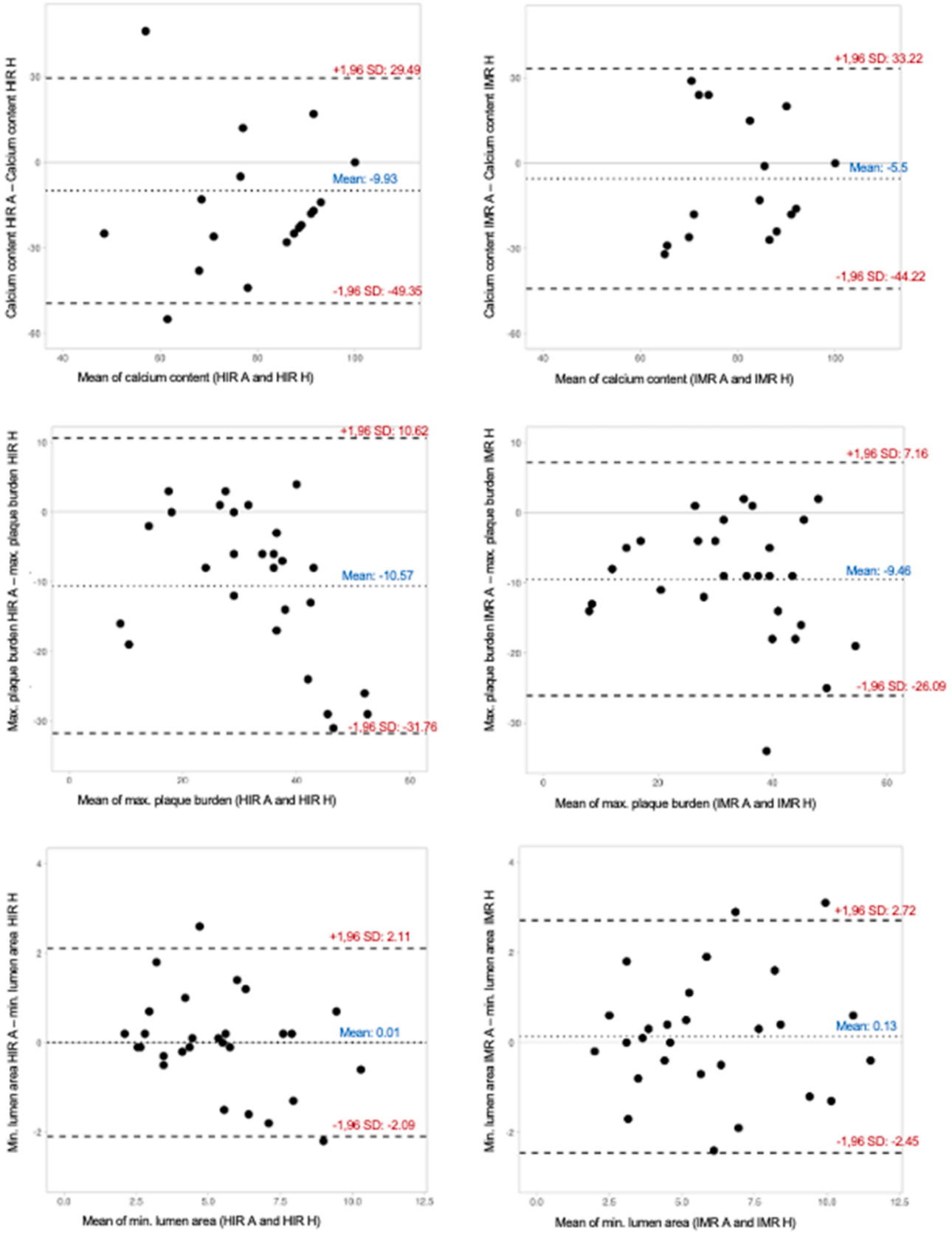

Fig. 6. Bland-Altman plots. Variability of calcium content (A), max. plaque burden (B) and min. lumen area (C) between the automatic measurements and the manual adjustment with HIR and IMR.

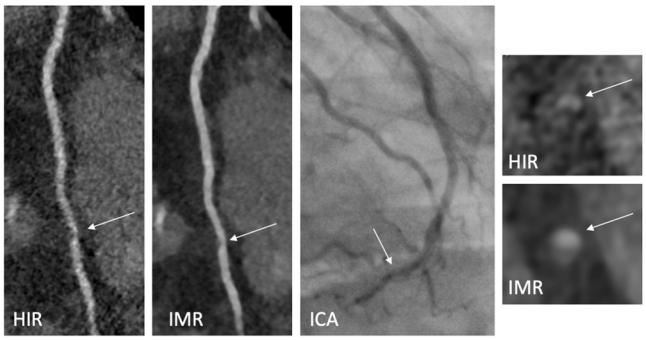

Fig. 7. Curved and axial reconstructions of the LAD with HIR and IMR reconstructions and ICA image. A false positive finding with HIR was observed in the patient who received a high radiation dose (DLP 477.6 mGycm) during CCTA. The HIR reconstruction showed high image noise accompanied by the detection of a significant stenosis in the distal LAD, while no significant stenosis was detected with the IMR and in the ICA.

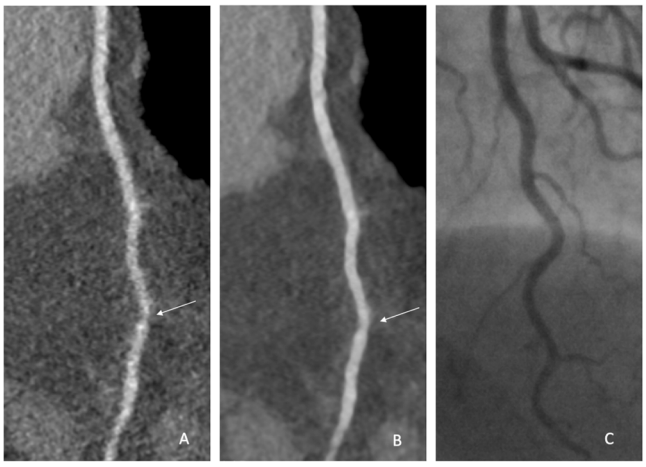

Fig. 8. Curved reconstructions of the LAD with HIR (A) and IMR (B) reconstructions and ICA image (C). The mild stenosis in the distal LAD segment appears to be more pronounced with HIR than with IMR. The manual diameter of the stenosis is 1 mm with HIR and 2.8 mm with IMR. In the ICA the stenosis is hardly traceable.

In clinical practice, this is particularly important for CCTA follow-up and the assessment of treatment response, when examinations are evaluated by different readers [21].

IMR reconstructions showed significantly steeper slopes of the FWHM curves than HIR, indicating significantly better contour sharpness and more accurate lumen diameter measurements. These results correlate with the findings of the study by Gassenmaier et al. who were able to demonstrate significantly better conspicuity of lumen edges on ADMIRE images in phantom experiments [10]. Additionally, sharper contour margins in IMR may improve the assessment of coronary stent patency [22].

Reduced image noise and improved image quality of IMR reconstructions over HIR were assumed to result in further impact on diagnostic accuracy. However, in our entire study population, the improvements with IMR did not reach statistical significance level. Further examination of the subgroups revealed that IMR exhibited a non-significant advantage over HIR in terms of diagnostic accuracy, regardless of image noise. Moreover, SNR did not significantly affect the sensitivity and specificity of either reconstruction. Our findings in adults align with Jia et al.'s study on infants with congenital heart defects [23] and another study on heavily calcified coronary arteries, where IMR demonstrated significantly superior diagnostic accuracy compared to FBP but similar results to HIR [5].

In patients who were exposed to higher radiation doses during CCTA, the diagnostic accuracy of IMR was indeed significantly superior to that of HIR. This was not due to superior sensitivity of IMR, but because HIR had reduced specificity at higher DLP values, leading to a greater number of false positive findings (Fig. 7). Since higher radiation doses are typically associated with larger examination volumes or obese patients, there is a risk that stenoses in these patients may be significantly overestimated when HIR is applied (Fig. 8). Further investigation of the BMI impact on CCTA revealed that IMR demonstrates markedly better sensitivity (89.47 %) compared to HIR (78.95 %). However, due to comparable specificity, PPV, and NPV, the overall diagnostic accuracy of HIR and IMR remained statistically indistinguishable. The divergent impact of BMI and DLP on the diagnostic accuracy of HIR and IMR of CCTA may be attributed to specific types of obesity and the distribution of mass in patients. The results of the Fisher's exact test indicated a trend for BMI to have impact on specificity of HIR and IMR ($p=0.19$ for HIR, $p=0.11$ for IMR).

In our quantitative plaque analysis was no statistically significant difference in minimal lumen area between automatic and manual contour marking, irrespective of the use of HIR or IMR. Additionally, there was excellent correlation between the reconstruction algorithms in both automatic and manual evaluation. However, a significantly larger minimum lumen area was measured on IMR images. As most plaques exhibited some degree of calcification, this is likely due to reduced calcium "blooming" artifacts on IMR images [24]. Therefore, IMR measurements may better reflect the true lumen area.

The role of CCTA in assessing suspected CAD is increasing, focusing on coronary plaque burden and plaque composition, which impact long-term cardiovascular outcomes [25]. Our quantitative plaque analysis revealed significantly higher amount of calcium in plaques on HIR images after manual adjustments compared to automatic detection. No such differences were found when IMR was applied. Adjusting the sensitivity of edge detection did not result in a significant improvement, unfortunately. Furthermore, the correlation between automated and manual plaque and lumen contour delineation was only weak to moderate for both reconstructions, aligning with R. A. Jonas et al.'s findings of high discordance between expert and AI-performed plaque component analysis [26]. Moreover, the software often failed to detect approximately one-third of plaque components, making it unreliable for plaque composition evaluation in clinical practice. IMR images provided more reliable minimum lumen area measurements than HIR, suggesting that automatic evaluation on IMR images could speed up stenosis analysis in clinical practice. However, further improvements of the tool are required for a complete and comprehensive automated plaque assessment.

IMR images have a different appearance compared to FBP or HIR images, often described as "waxy" or "plastic" [27]. For this reason, radiologists need to adapt to the new and special appearance of IMR images, which may initially limit the diagnostic confidence, especially for inexperienced evaluators. In our study, differing levels of prior experience with HIR and IMR among observers may have contributed to the "only" substantial inter-observer agreement. To eliminate these discrepancies, various vendors have developed several deep learning-based image reconstruction methods that reduce noise and improve spatial resolution and object recognizability without altering the texture [28].

Our study has the following limitations: First, despite the consensus reached following the evaluation, discrepancies may have occurred when determining to which segment the stenosis belongs. This is particularly relevant in the stenosis of the RCA and the LAD, as the RCA is divided into a proximal, middle, and distal third. Similar issues may have arisen in the case of the LAD if the stenosis was situated at a segment boundary. Second, there is selection bias as all patients included in the study had undergone CCTA for suspected CAD and had already been referred for further investigation for ICA. The prevalence of the disease in the selected patient population was higher than in the

total collective of all patients referred for CCTA during the study period including the majority of those without need for ICA. Third, all segments of coronary arteries with a diameter greater than 1.8 mm were equally included in the study without consideration of the localization of the stenosis along the vessel or clinical relevance. Fourth, the segment-based evaluation of coronary artery stenoses for the entire study cohort was visually graded according to the CAD-RADS classification [12]. A quantitative plaque analysis was performed just on 28 selected and suitable plaques. Fifth, all CCTA examinations were performed on a single CT device and processed and analyzed with a single software program. Finally, it should be noted that the study is limited by its retrospective, monocentric nature.

5. Conclusions

IMR offers significantly superior image quality of CCTA, sharper coronary contours with more precise measurements, a stronger positive correlation with ICA, and slightly better interobserver agreement than HIR. The overall diagnostic accuracy may be superior when using IMR, although the differences were not statistically significant. However, in patients who are exposed to higher radiation doses during CCTA due to their constitution, IMR enables significantly better diagnostic accuracy than HIR thus providing a specific benefit for obese patients. IMR demonstrates a high degree of correlation between the automatic and manual evaluations in the assessment of the minimum lumen area, thereby providing more accurate measurements than HIR.

Funding

This research received no specific grant from any funding agency in the public, commercial, or not-for-profit sectors.

Ethical Statement

Ethical approval for this study was waived by the ethics committee of the Bavarian Medical Association because of the retrospective study design.

CRediT authorship contribution statement

Verena Bauer: Investigation. **Aiste Matuleviciute-Stojanoska:** Writing – review & editing, Writing – original draft, Visualization, Validation, Resources, Methodology, Investigation, Formal analysis, Conceptualization. **Julia Sautier:** Investigation. **Christian Stumpf:** Writing – review & editing, Supervision. **Thorsten Klink:** Writing – review & editing, Supervision, Project administration, Methodology, Investigation, Formal analysis, Data curation. **Martin Nuessel:** Investigation. **Volha Nizhnikava:** Methodology, Investigation.

Declaration of Competing Interest

The authors declared no conflict of interests related to the manuscript.

References

[1] B.B. Hoorweg, R.T. Willemsen, L.E. Cleef, T. Boogaerts, F. Buntinx, J.F. Glatz, G. J. Dinant, Frequency of chest pain in primary care, diagnostic tests performed and final diagnoses, Heart 103 (21) (2017) 1727–1732.
[2] K.B.K. Bundesärztekammer (BÄK), Arbeitsgemeinschaft der Wissenschaftlichen Medizinischen Fachgesellschaften (AWMF). Nationale VersorgungsLeitlinie. Chronische KHK, Version 6.0., 2016. (Accessed 2022.11.19.
[3] F.R. de Graaf, J.D. Schuijf, J.E. van Velzen, L.J. Kroft, A. de Roos, J.H. Reiber, E. Boersma, M.J. Schalij, F. Spanó, J.W. Jukema, E.E. van der Wall, J.J. Bax, Diagnostic accuracy of 320-row multidetector computed tomography coronary angiography in the non-invasive evaluation of significant coronary artery disease, Eur. Heart J. 31 (15) (2010) 1908–1915.
[4] L. Ru, P. Lan, C. Xu, L. Lu, T. Chen, The value of coronary CTA in the diagnosis of coronary artery disease, Am. J. Transl. Res 13 (5) (2021) 5287–5293.
[5] J. Kim, B.S. Goo, Y.S. Cho, T.J. Youn, D.J. Choi, A. Dhanantwari, M. Vembar, E. J. Chun, Diagnostic performance and image quality of iterative model-based reconstruction of coronary CT angiography using 100 kVp for heavily calcified coronary vessels, PLoS One 14 (9) (2019) e0222315.
[6] D. Ippolito, L. Riva, C.R. Talei Franzesi, C. Cangiotti, A. De Vito, F. Di Gennaro, G. D'Andrea, A. Crespi, S. Sironi, Diagnostic efficacy of model-based iterative reconstruction algorithm in an assessment of coronary artery in comparison with standard hybrid-Iterative reconstruction algorithm: dose reduction and image quality, Radio. Med 124 (5) (2019) 350–359.
[7] T. Klink, V. Obmann, J. Heverhagen, A. Stork, G. Adam, P. Begemann, Reducing CT radiation dose with iterative reconstruction algorithms: the influence of scan and reconstruction parameters on image quality and CTDIvol, Eur. J. Radio. 83 (9) (2014) 1645–1654.
[8] H. Precht, O. Gerke, J. Thygesen, K. Egstrup, S. Auscher, D. Waaler, J. Lambrechtsen, Image quality in coronary computed tomography angiography: influence of adaptive statistical iterative reconstruction at various radiation dose levels, Acta Radio. 59 (10) (2018) 1194–1202.
[9] M.J. Cha, J.S. Seo, D.S. Yoo, S. Chong, Knowledge-based iterative model reconstruction in coronary computed tomography angiography: comparison with hybrid iterative reconstruction and filtered back projection, Acta Radio. 59 (3) (2018) 280–286.
[10] T. Gassenmaier, I. Distelmaier, A.M. Weng, T.A. Bley, T. Klink, Impact of advanced modeled iterative reconstruction on interreader agreement in coronary artery measurements, Eur. J. Radio. 94 (2017) 201–208.
[11] H.K. Lapp, Ingo, Das Herzkatheterbuch, Thieme (2014).
[12] R.C. Cury, J. Leipsic, S. Abbara, S. Achenbach, D. Berman, M. Bittencourt, M. Budoff, K. Chinnaiyan, A.D. Choi, B. Ghoshhajra, J. Jacobs, L. Koweek, J. Lesser, C. Maroules, G.D. Rubin, F.J. Rybicki, L.J. Shaw, M.C. Williams, E. Williamson, C. S. White, T.C. Villines, R. Blankstein, CAD-RADS 2.0 - 2022 coronary artery disease-reporting and data system: an expert consensus document of the Society of Cardiovascular Computed Tomography (SCCT), the American College of Cardiology (ACC), the American College of Radiology (ACR), and the North America Society of Cardiovascular Imaging (NASCI), J Cardiovasc. Comput. Tomogr. 16 (6) (2022) 536–557.
[13] D.G. Altman, J.M. Bland, Diagnostic tests 3: receiver operating characteristic plots, BMJ 309 (6948) (1994) 188.
[14] J.R. Landis, G.G. Koch, The measurement of observer agreement for categorical data, Biometrics 33 (1) (1977) 159–174.
[15] M.M. Mukaka, Statistics corner: a guide to appropriate use of correlation coefficient in medical research, Malawi Med J. 24 (3) (2012) 69–71.
[16] J.G.U. Graham, Fisher's exact test, J. R. Stat. Soc. Ser. A (Stat. Soc.) 155 (3) (1992) 395–402.
[17] Y.H. Chan, Biostatistics 104: correlational analysis, Singap. Med J. 44 (12) (2003) 614–619.
[18] J.M. Bland, D.G. Altman, Statistical methods for assessing agreement between two methods of clinical measurement, Lancet 1 (8476) (1986) 307–310.
[19] E.R. DeLong, D.M. DeLong, D.L. Clarke-Pearson, Comparing the areas under two or more correlated receiver operating characteristic curves: a nonparametric approach, Biometrics 44 (3) (1988) 837–845.
[20] L. Qin, Z. Ma, F. Yan, W. Yang, Iterative model reconstruction (IMR) algorithm for reduced radiation dose renal artery CT angiography with different tube voltage protocols, La Radiol. Med. 123 (2) (2018) 83–90.
[21] R. Symons, J.Z. Morris, C.O. Wu, A. Pourmorteza, M.A. Ahlman, J.A. Lima, M. Y. Chen, M. Mallek, V. Sandfort, D.A. Bluemke, Coronary CT angiography: variability of CT scanners and readers in measurement of plaque volume, Radiology 281 (3) (2016) 737–748.
[22] T. Hickethier, B. Baessler, J.R. Kroeger, D. Muller, D. Maintz, G. Michels, A. C. Bunck, Knowledge-based iterative reconstructions for imaging of coronary artery stents: first in-vitro experience and comparison of different radiation dose levels and kernel settings, Acta Radio. 60 (2) (2019) 160–167.
[23] Q. Jia, J. Zhuang, J. Jiang, J. Li, M. Huang, C. Liang, Image quality of ct angiography using model-based iterative reconstruction in infants with congenital heart disease: comparison with filtered back projection and hybrid iterative reconstruction, Eur. J. Radio. 86 (2017) 190–197.
[24] M. Renker, J.W. Nance Jr., U.J. Schoepf, T.X. O'Brien, P.L. Zwerner, M. Meyer, J. M. Kerl, R.W. Bauer, C. Fink, T.J. Vogl, T. Henzler, Evaluation of heavily calcified vessels with coronary CT angiography: comparison of iterative and filtered back projection image reconstruction, Radiology 260 (2) (2011) 390–399.
[25] D.A. Halon, I. Lavi, O. Barnett-Griness, R. Rubinshtein, B. Zafrir, M. Azencot, B. S. Lewis, Plaque morphology as predictor of late plaque events in patients with asymptomatic type 2 diabetes: a long-term observational study, JACC: Cardiovasc. Imaging 12 (7, Part 2) (2019) 1353–1363.
[26] R.A. Jonas, S. Weerakoon, R. Fisher, W.F. Griffin, V. Kumar, H. Rahban, H. Marques, R.P. Karlsberg, R.S. Jennings, T.R. Crabtree, A.D. Choi, J.P. Earls, Interobserver variability among expert readers quantifying plaque volume and plaque characteristics on coronary CT angiography: a CLARIFY trial sub-study, Clin. Imaging 91 (2022) 19–25.
[27] R.C. Nelson, S. Feuerlein, D.T. Boll, New iterative reconstruction techniques for cardiovascular computed tomography: how do they work, and what are the advantages and disadvantages? J. Cardiovasc. Comput. Tomogr. 5 (5) (2011) 286–292.
[28] C. Park, K.S. Choo, Y. Jung, H.S. Jeong, J.Y. Hwang, M.S. Yun, CT iterative vs deep learning reconstruction: comparison of noise and sharpness, Eur. Radio. 31 (5) (2021) 3156–3164.